

REVISION #1

Solid solution in the apatite OH-Cl binary system: compositional dependence of solid solution mechanisms in calcium phosphate apatites along the Cl-OH binary

JOHN M. HUGHES^{1,*}

¹Department of Geology, University of Vermont, Burlington, Vermont 05405, U.S.A.

DANIEL HARLOV^{2,3}

²GeoForschungsZentrum Potsdam, Telegrafenberg, D-14473 Potsdam, Germany

³Department of Geology, University of Johannesburg P.O. Box 524, Auckland Park, 2006
South Africa

SEAN R. KELLY⁴, JOHN RAKOVAN⁴

⁴Department of Geology and Environmental Earth Science, Miami University, Oxford, Ohio 45056,
U.S.A.

MAX WILKE²

²GeoForschungsZentrum Potsdam, Telegrafenberg, D-14473 Potsdam, Germany

ABSTRACT

The method of accommodation of solid solution along the OH-Cl binary in calcium phosphate apatites is not fully understood; because of steric constraints in mixtures of OH and Cl anions in the apatite [0,0,z] anion column, the positions of OH and Cl anions in the pure hydroxylapatite and chlorapatite endmembers cannot coexist in the binary anion column. We

* E-mail: jmhughes@uvm.edu

have undertaken high-precision single-crystal X-ray structure studies of eight synthetic samples along the OH-Cl apatite binary ($R_1 \leq 0.0159$). We found that for all samples solid solution is attainable in space group $P6_3/m$, but the particular method of solid solution is dependent on composition. For samples with $\text{Cl} > \text{OH}$, three column anion sites (two for Cl, one for OH) provide allowable bond distances with the Ca₂ atoms and allow a sequence of column anions that provides sufficient anion-anion distances and also effects reversal of the sense of ordering of the column anions relative to the mirror planes at $z = 1/4$ and $3/4$. In a sample with $\text{OH} > \text{Cl}$, three sites exist in the anion column that also provide allowable bond distances to the triangle of Ca₂ atoms or its disordered Ca₂' equivalent, and afford a sequence of atoms that permits reversal of the anion column and maintenance of $P6_3/m$ symmetry. One of those sites is occupied by OH, and provides acceptable Ca₂-OH distances, and another accommodates Cl with ideal Ca₂-Cl distances. A third column anion site is unique among the calcium phosphate apatites. That site, termed the ClOH site, accommodates *both* OH and Cl. The site has an ideal bond distance for OH to the Ca₂ atoms in the Ca₂ triangle, and also has an ideal bond distance for a Cl occupant to disordered Ca₂' atoms; thus, because of the disordering of the Ca₂-Ca₂' atoms, a single site can accommodate either anion with ideal, but disparate, bond distances to Ca. Finally, in OH-Cl apatites with $\text{OH} \approx \text{Cl}$, also crystallizing in space group $P6_3/m$, four anion positions are occupied in the anion column, including the ClOH site that allows occupancy by both OH and Cl. In addition to that site and distinct OH and Cl sites, OH is found to occupy the site within the mirror plane at (0,0,1/4), the site occupied by F in F-bearing apatite. Occupancy of that site is essential to reversing the sense of ordering of the anion column relative to the mirror planes and preserving $P6_3/m$ symmetry. Thus, the methods of effecting solid solution along the OH-Cl are composition-dependent and complex.

Keywords: apatite, hydroxylapatite, chlorapatite, solid solution, binary, crystal structure

INTRODUCTION

Apatite is the most abundant phosphate mineral on Earth and a phase with fundamental importance in geology, agriculture, materials science, medicine and dentistry. In addition to the apatite that forms in igneous, metamorphic, sedimentary, and hydrothermal environments, all hard tissue of the human body except small parts of the inner ear is formed of apatite materials, indicating a remarkable link between the inorganic and organic genesis for the mineral; apatite is among the few most common biominerals on Earth. In addition, apatite forms the foundation of the global phosphorus cycle. The importance of apatite in many disciplines, indeed in even sustaining human life as the chief source of phosphate for fertilizer, cannot be overstated. The reader is referred to a recent *Elements* issue (V. 11, June, 2015) that is devoted entirely to apatite for a more detailed account of the chemistry, structure, and applications of the mineral.

Apatite *sensu lato* has a composition of $\text{Ca}_{10}(\text{PO}_4)_6(\text{OH},\text{F},\text{Cl})_2$, and is one of the more rare *anion* solid solutions among minerals. Despite the importance and ubiquitous nature of the mineral, details of the apatite atomic arrangement have not been forthcoming. Hughes et al. (1989) demonstrated that the positions of the $[0,0,z]$ column anions in the apatite end-members (fluorapatite, chlorapatite, and hydroxylapatite) are not compatible in solid solution because of steric constraints. This has led to speculation on how solid solution is effected in apatite *sensu lato*, but definitive structures on all the binaries are not extant. Hughes (2015) summarized the apatite atomic arrangement and the state of our knowledge of the apatite structure, and illustrated

the conundrum of the steric constraints among the anions. We refer the reader to that work for a summary of the apatite atomic arrangement.

For any combination of anion occupants, the positions of the anions in the [0,0,z] anion column result from several factors, including the size of the particular column anions, the nearest-neighbors in the anion column and electrostatic repulsions therefrom, any dissymmetrization that is present in the structure, electrostatic attractions to the surrounding triangle of Ca₂ atoms, and, in hydroxylapatite, the hydrogen bonding that occurs from the hydroxyl hydrogen to neighboring column anions. Hughes et al. (1990) demonstrated that in ternary apatite, solid solution among all three column anions was achieved in two different ways. They examined a low-temperature, metamorphic apatite that accommodated all three column anions by reducing the typical hexagonal $P6_3/m$ apatite symmetry to monoclinic $P2_1/b$ symmetry, a dissymmetrization resulting from ordering of the anions. In a high-temperature volcanic apatite, they demonstrated that accommodation of all three column anions is made possible by occupation of a second Cl site, one not seen in the pure chlorapatite end-member, a site that shifts the Cl atom closer to its associated mirror plane and provides sufficient distance for a neighboring hydroxyl. A sequence of anions can thus be erected that allows sufficient distance between all nearest-neighbors in the anion column and also allows reversal of the sense of local order relative to the mirror planes at [0,0,1/4] and [0,0,3/4] (column reversal), thus effecting the $P6_3/m$ symmetry over the crystal as a whole.

Although the accommodation of three anions in the apatite anion column has been illustrated, the anion positions along the three binary joins in the F-OH-Cl apatite ternary are more problematic (McCubbin et al. 2008). Hughes et al. (2014a) showed that in synthetic $P6_3/m$ F-Cl apatite, the two disparate ions are accommodated by the creation of an off-mirror fluorine

site that allows sufficient anion-anion distances and also allows column reversal; Hughes et al. (2014b) also showed that a natural F-Cl analog with the same anion accommodation method occurs in the Three Peaks area of Utah.

Young et al. (1969) investigated the accommodation of anions in F-OH binary apatite using nuclear magnetic resonance spectroscopy. They noted that in the anion column the fluorine atom shifts at least 0.1\AA off the mirror plane when in an environment of asymmetric hydrogen bonding. Their study demonstrated that asymmetric hydrogen bonding (OH-F) or symmetric hydrogen bonding (OH-F-HO) “secures” the F more strongly in the anion column, and this enhanced bond strength inhibits hydroxyl diffusion along the anion column. They invoked this fact to explain the observation that solubility of hydroxylapatite decreases with substituent fluorine in the anion column, as diffusion of hydroxyl is a component of dissolution of apatite; such an observation is particularly germane in the fluoridation of tooth enamel as a prophylaxis for dental caries.

The accommodation of OH and Cl in the binary apatite anion column is less well understood. The positions of the anions in the endmembers do not provide an atomic arrangement that yields sufficient distances between the anions nor does it provide a mechanism for column anion reversal. Garcia-Tunon et al. (2012) also undertook a study on synthetic apatite, and described a model for accommodation of the two anions in the binary anion column. However, the use of anisotropic thermal parameters for the column anions, as employed in that study, creates difficulties in refinement by obscuring sites with small occupancy by large values of U_{33} of other column anions (Hughes et al. 2014a), and thus the present study was undertaken.

To determine the structural compatibility of any two anions in the apatite anion column, we have synthesized crystals along the three binaries in the (F-OH-Cl) apatite ternary system and

undertaken single-crystal X-ray structure studies on those crystals. Here we report the atomic arrangements of members of the OH-Cl binary, and illustrate the several ways that solid solution can be effected. The compositions of the studied crystals along the OH – Cl binary are illustrated in Figure 1.

SOLID SOLUTION APATITE BINARIES: THE CONUNDRUM

The radii of the three occupants of the apatite anion columns ($F = 1.30\text{\AA}$, Shannon and Prewitt 1969; $Cl = 1.72\text{\AA}$, $OH = 1.33\text{\AA}$; Jenkins and Thakur 1979) differ greatly, with Cl being much larger than F and OH. In addition the three anions exist in $[0,0,z]$ columns at the edges of the unit cells, and those columns are intersected by $\{0,0,\ell\}$ mirror planes at $z = \frac{1}{4}$ and $\frac{3}{4}$ (Figure 2). Most commonly, the apatite compounds are hexagonal, crystallizing in space group $P6_3/m$, but trigonal and monoclinic subsymmetries do exist in more rare apatite compounds (Hughes and Rakovan 2015).

Where F occupies the anion column, it occurs in a site that is contained within the mirror plane, at $(0,0,\frac{1}{4})$ or $(0,0,\frac{3}{4})$; that site is surrounded by a triangle of Ca2 atoms. For OH- or Cl-bearing apatites, however, the OH and Cl column anions are too large to fit in the center of the triangle of Ca2 atoms. Thus, the hydroxyls are displaced $\sim 0.35\text{\AA}$ above *or* below its associated mirror plane, and the larger Cl atoms are displaced $\sim 1.3\text{\AA}$ above *or* below its associated mirror plane. Therefore, with an F atom site, true mirror symmetry is maintained in each unit cell; at OH- and Cl-occupied sites, although local mirror symmetry is not present at any mirror plane, average mirror symmetry is attained over the crystal as a whole, as the OH and Cl sites above and below the mirror plane are all half-occupied. This is only strictly true when OH or Cl are disordered, above and below the mirror, over the entire structure.

In apatites that contain mixtures of the column anions, if indeed they crystallize in space group $P6_3/m$, the sequence of column anions must allow for reversals of the sense of ordering in the anion column, i.e., allow for reversal of anions from ordered above the plane to below the plane, and the converse, and also provide sufficient anion-anion distances for coexistence of column anions. Figure 3 illustrates the conundrum by showing the maximum anion-anion distances in the anion column that can be achieved using the anion positions in the hydroxylapatite and chlorapatite hexagonal endmembers (Hughes et al. 1989). Clearly, the endmember OH and Cl anion positions are not compatible in the OH-Cl binary column, yielding a Cl-O(H) distance of 2.53 Å and an H-H distance of 0.83 Å.

Below we describe the synthesis of samples along the OH-Cl binary, provide the details of the crystal structure studies of their atomic arrangements, and illustrate how the criteria for $P6_3/m$ symmetry are met for three different ranges of composition along the OH-Cl calcium apatite binary.

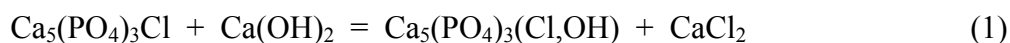
Synthesis of apatite samples

Apatites across the Cl-OH join were synthesized utilizing Cl-OH exchange between synthetic pure end member chlorapatite and a series of $\text{Ca}(\text{OH})_2\text{-H}_2\text{O}$ solutions at 1100 °C and 400 MPa. Synthesis of a large size range of chlorapatite crystals up to 5 or more mm in length was achieved by dry mixing 0.03 moles (9.3 grams) of $\text{Ca}_3(\text{PO}_4)_2$ into 0.1 moles of CaCl_2 (11 grams). This mix was taken up to 1375 °C in a covered Pt crucible in open air, soaked at 1375 °C for 15 hours, and then slowly cooled to 1220 °C at 3 °C per hour after which the crucible was removed from the oven and air cooled (see Schettler et al. 2011). The chlorapatite crystals were

released from the flux by boiling the crystal/flux mass in 2 liters of distilled H₂O followed by several additional washings.

Apatites across the Cl-OH join were then synthesized by exchanging 400 mg of a 200 – 500 µm size separate of these synthetic chlorapatites with 25 – 200 mg of a Ca(OH)₂-H₂O solution with variable proportions of Ca(OH)₂ and H₂O. Each of the chlorapatite-Ca(OH)₂-H₂O mixes were sealed in a 4 cm long, 5 mm diameter Pt capsule and taken up to 1100 °C and 400 MPa in an internally heated gas pressure vessel using Ar as the pressure medium. Run duration was 3 – 6 days. The temperature was measured with 3 S-type thermocouples and calibrated based on measurements of the melting points of NaCl at 843 °C/200MPa and 904 °C/500 MPa (Akella et al. 1969). The accuracy is about ±5 °C at 200 MPa and ± 20 °C at 500 MPa. Maximum thermal gradients along the capsules were ±10 °C. Pressure measurement was done with a strain gauge and was accurate to ±7 MPa for experiments up to 500 MPa. During the experiment, pressure was controlled automatically within ±5 MPa using the hydraulic system of the intensifier and a programmable control unit. The samples were heated isobarically with a rate of 30 °C/min and quenched isobarically with quench rates of 150–200 °C/min.

During the experiment the following total exchange took place between the chlorapatite crystals and the Ca(OH)₂-H₂O solution via a coupled dissolution-reprecipitation process (see Putnis 2009):



and



After quench the Pt capsule was opened and the exchanged Cl-OH apatites removed and washed 4 – 5 times in a 100 ml beaker of doubly distilled H₂O at room temperature to remove

the CaCl_2 , HCl, and whatever $\text{Ca}(\text{OH})_2$ remained. The washed Cl-OH apatite crystals were then air dried at room temperature.

Details of X-ray structure studies

X-ray diffraction data were collected with a Bruker Apex II CCD single-crystal diffractometer using graphite-monochromated Mo K_α radiation; complete details of crystal data and data collection, results of the structure studies, and cif files for each of the eight crystals described herein have been deposited.² For each sample, redundant data were collected for a sphere of reciprocal space (4,500 frames, 0.20° scan width; average redundancy \approx 16) and were integrated and corrected for Lorentz and polarization factors and absorption using the Bruker Apex2 package of programs. The atomic arrangement was refined in space group $P6_3/m$, on F^2 , with SHELXL-97 (Sheldrick 2008) using neutral atom scattering factors and full-matrix least-squares, minimizing the function $\sum w(F_o^2 - F_c^2)^2$ with no restraints. All atoms were refined with anisotropic temperature factors except the column anions; an extinction coefficient was also refined. As noted previously, in earlier studies it was found that the use of anisotropic atomic displacement factors for the column anions yields unreasonable values of U_{33} , an anisotropy that masks the positions of anion sites occupied by small fractions of a column anion. The occupancy values of the column anions were not constrained.

² Deposit items AM-16-xx1 for crystal data and data collection conditions, AM-16-xx2 for positions of atoms and equivalent isotropic atomic displacement parameters, and AM-16-xx3 for CIF files, respectively. Deposit items are available two ways: for paper copies contact the Business Office of the Mineralogical Society of America (see inside front cover of recent issue) for price information. For an electronic copy visit the MSA web site at <http://www.minsocam.org>, go to the *American Mineralogist* Contents, find the table of contents for the specific volume/issue wanted, and then click on the deposit link there.

After initial refinements of the structure, the column anion positions were located using difference maps. In addition to those peaks, in many of the structures the largest peak in the difference map was located near the Ca2 atom, suggesting that the peak resulted from disorder of Ca2 in response to the different local bonding environments provided by the adjacent column anions, a common occurrence in apatites with mixed occupants in the anion column (Hughes *et al.* 1990). That disorder was successfully modeled in the structures where the Ca2' peak was noted (i.e., all structures with $\text{OH} \approx \text{Cl}$ and $\text{OH} > \text{Cl}$).

As will be described subsequently, there is a partially occupied site in the anion column that can contain either Cl or OH because of disorder of the surrounding Ca2 atoms, termed the ClOH site. To model occupancy of that site, the site occupancy was first refined with Cl scattering factors. Because we were thus modeling a site with mixed O(H) and Cl occupancy, modeling that site with Cl atoms invariably yielded a total anion column occupancy less than the necessary 2.00 *apfu*, and modeling the electron occupancy with O(H) invariably led to a total anion occupancy greater than 2.00. We then determined how many atoms were needed to fill the anion column to 2.00 *apfu*, and apportioned the electron occupancy of that site to a combination of O(H) and Cl that maintained the total electron occupancy and filled the anion column to 2.00 *apfu*. The validity of the assumption of a full anion column is demonstrated by the refinement of three of the samples *without* a ClOH site, which yielded total anion column occupancy of 2.02, 2.04, and 2.01 anions in unconstrained refinements.

RESULTS OF THE STRUCTURE STUDIES

The results of the structure studies of the crystals along the OH-Cl apatite binary suggest the accommodation of OH and Cl can occur in three ways, depending on the composition of the

binary apatite. Below we summarize those accommodations and illustrate the column anion arrangement in apatites along the OH-Cl binary. First, however, a few comments on disorder in the apatite structure are appropriate.

The anion columns in apatite are surrounded by a triangle of Ca₂ atoms (Fig. 2). As the column anions vary within the apatite anion column, it has been shown (Sudarsanan and Young, 1978; Hughes et al., 1990) that the Ca₂ atoms in the triangle can disorder into a second position, herein called Ca₂' , to respond to the particular nearest-neighbor column anion, with Ca₂-Ca₂' distances on the order of 0.3Å. In the structures in this paper in which the Ca₂' position was among the three largest difference peaks in the penultimate Fourier electron density difference map, we modeled the Ca₂' site in the structure. That disorder also propagates to oxygen atoms, particularly O₃. However, disorder of oxygen atoms that propagates from disorder of the Ca₂ atoms is difficult to model in part due to their relatively small scattering factors, and thus oxygen disorder was not modeled in this study. The disorder of the Ca₂ atoms is particularly important in creating a unique anion column site, as will be explained subsequently.

BINARY APATITES WITH Cl > OH.

We examined three samples of OH - Cl apatite that have Cl > OH (Figure 1). The contents of the anion columns in these crystals, as determined by the single-crystal structure refinements, are [Cl_{1.65}(OH)_{0.37}] (sample APS78), [Cl_{1.66}(OH)_{0.38}] (sample APS82), and [Cl_{1.75}(OH)_{0.26}] (sample APS83). The samples provided superior refinements, with *R*₁ values of 0.0157, 0.0148, and 0.0158, respectively. In those samples, we found the symmetry is indeed hexagonal, *P*6₃/*m*; reversal of the anion column to achieve this hexagonal symmetry occurs with a single O(H) site and two Cl sites. We have deposited the complete details of the data

collection, structure refinement and results of the structure studies for these samples APS78, APS82, and APS83. For the reader's convenience, Table 1 contains the atomic coordinates and equivalent atomic displacement parameter for one of the samples, APS83, and the interatomic distances we note below are from that sample.

The anion column reversal sequence for apatites along the OH-Cl binary with compositions with Cl > OH is depicted in Figure 4, and the z coordinates of the column anion sites and their percentage of the total occupancy are given in Table 2. As seen in Table 2, three positions exist in the anion column, two of which accommodate Cl atoms and one that accommodates OH occupants. In the apatites with Cl > OH, the OH anion is located at a single site at $z \approx 0.183$, slightly farther from the mirror plane than in endmember hydroxylapatite; that OH bonds to three Ca₂ atoms at 2.525 Å distance. Cl is accommodated in a site at $z \approx 0.06$ (labeled Cl_a), similar to the location in hexagonal chlorapatite, and bonds to three Ca₂ atoms at distances of 2.812 Å. A second Cl site (Cl_b) at $z \approx 0.105$ also presents a bonding environment that accommodates Cl, at a distance of 2.677 Å from each of three Ca₂ atoms. In the three samples analyzed with Cl > OH, the occupancy of the two Cl sites demonstrates that approximately twice as many Cl_a sites are occupied as Cl_b sites.

The anion column depicted in Figure 4 illustrates an anion sequence that allows reversal of the anion column and acceptable anion-anion distances. The minimum 3.08 Å Cl-Cl distance is at the lower end of observed Cl-Cl distances in a recent compilation (~3.0 - ~4.0 Å; Vener et al. 2013), but is within the range of observed Cl-Cl contacts. The other distances that are derived from this set of anion column sites are an OH-Cl distance of 2.85 Å and an OH-OH distance of 2.49 Å. The latter distance is somewhat short for an O-O distance, but in the range typical for a hydrogen bonded O-H...O distance with strong hydrogen bonding. Brown (1976) distinguishes

between weak hydrogen bonds ($O-O > 2.7\text{\AA}$) and strong hydrogen bonds ($O-O < 2.7\text{\AA}$), and noted that the strong hydrogen bonds tend to be linear and weak hydrogen bonds tend to be bent. In the apatite anion column, the hydrogen bonds will always be linear, and thus the observed O-O distance, that we assume is hydrogen bonded, is of an ideal distance. Although in this work we have not located the H atoms in the column hydroxyls, we can thus suggest that hydrogen bonding occurs between two adjacent hydroxyls to yield the 2.49\AA OH-OH distance. We comment subsequently on hydrogen bonding in the OH - Cl apatite anion column.

It is of interest to note, and germane to the other methods of column reversal along the OH - Cl apatite anion column for compositions of $OH \approx Cl$ and $OH > Cl$, that there is no disordering of the Ca2 atom detected in the structures with $Cl > OH$. As will be illustrated subsequently, that disorder is necessary for the other methods of accommodation of column reversal, but not for the configuration in samples with $Cl > OH$.

BINARY APATITES WITH $OH > Cl$.

We have synthesized a single sample with $OH > Cl$, and we found it has a method of reversing the anion sequence and preserving $P6_3/m$ hexagonal symmetry in the OH-Cl apatite anion column that has not been previously recognized. We have deposited the complete details of the data collection, structure refinement and results of the structure studies for sample APS76. For the reader's convenience, Table 3 contains the atomic coordinates and equivalent atomic displacement parameter for the sample; the sample provided a superior refinement, with $R_1 = 0.0149$. Note that sample APS76 contains disordered Ca2 atoms, as a portion of the Ca2 atoms are disordered into Ca2' sites approximately 0.3\AA distant.

Table 4 lists the z coordinates of the $(0,0,z)$ column anion positions as well as the portion of each site that is occupied. As seen in Table 4, a column anion site occurs at $z = 0.154$ (labeled ClOH), a column anion site not previously recognized in any apatite study and a site approximately midway between endmember Cl sites and OH sites. Accompanying that site are an OH site at $z = 0.202$ (2.381 Å distant from Ca₂), essentially at the OH site found in endmember hydroxylapatite, and a Cl_b site at $z = 0.083$ (2.623 Å distant from Ca₂), near the Cl site in endmember chlorapatite.

The reversal of the anion column using these sites to facilitate $P6_3/m$ symmetry is illustrated in Figure 5. Of particular interest in the OH-Cl binary anion column is the newly discovered ClOH site. As mentioned and referenced previously, the Ca₂ atoms in apatites with more than one column anion can disorder to allow the Ca₂ atoms to occupy positions that provide ideal bond distances to the particular column anion (F, OH, Cl) associated with the mirror plane that contains the Ca₂ (Ca₂') triangle. Along the OH-Cl binary, with samples that contain OH > Cl, the ClOH site occupies a unique position that accommodates *both* Cl and OH at ideal bond distances with the surrounding Ca₂ triangle, one anion at an ideal bond distance with Ca₂, and the other at an ideal bond distance with the disordered Ca₂' atoms.

The ClOH position at $z = 0.154$ in sample APS76, with OH > Cl, provides a bond distance between the Ca₂ site and O(H) occupying the ClOH site of 2.45 Å, and the disordered Ca₂' atom has a bond distance of 2.72 Å to a Cl atom in the ClOH site. Both bond distances are nearly ideal for the respective anions to Ca; thus, a single column anion site can accommodate both Cl and OH at ideal bond distance to the neighboring Ca₂ atoms, with O(H) bonding to a Ca atom and Cl bonding to its disordered equivalent Ca₂' atom. This is the first time such a site has been

observed in the apatite anion column, and serves to illustrate the robust nature of accommodation of column anions in the apatite atomic arrangement.

BINARY APATITES WITH OH \approx Cl.

We have synthesized four samples with OH \approx Cl in the OH-Cl apatite column (Figure 1). Those samples, like those with OH > Cl and Cl > OH, present a unique method of reversing the sequence of the anion column and preserving $P6_3/m$ symmetry. We have deposited the complete details of the data collection, structure refinement and results of the structure studies for these samples APS71 ($R_1 = 0.0159$), APS72 ($R_1 = 0.0151$), APS74 ($R_1 = 0.0155$), and APS80 ($R_1 = 0.0155$). For the reader's convenience, Table 5 contains the atomic coordinates and equivalent atomic displacement parameter for one of the samples, APS71, and the interatomic distances we note below are from that sample. Table 6 lists the z coordinates and percentage occupancy for the four occupied sites in the anion column; that set of occupied sites is unique in the calcium phosphate apatites.

Figure 6 depicts the method of reversal of the anion column in the OH-Cl anion column with OH \approx Cl. As illustrated there and listed in Table 6, there is a Cl site (Cl_a) at (0,0,0) in which a small portion of the sites are occupied (< 5% on average of the structures studied); this site is occupied by Cl in the F-Cl binary apatites (Hughes et al. 2014a) but was not previously noted in OH-Cl binary apatites. Because the position of that Cl atom is halfway between two mirror planes ($z = -1/4$, $z = +1/4$), Cl atoms in that site bond to six Ca2 atoms rather than three, leading to longer Ca2-Cl bond lengths (Ca2- Cl_a distance = 2.908Å) that are sufficient to match the bond valence sum of the Cl.

We can suggest that the Cl site at (0,0,0) is partially occupied by OH, in a mechanism suggested by Mackie and Young (1974). In their deduction of anion positions in the fluor-chlorapatite anion column, Mackie and Young suggested three criteria, paraphrased here: 1) the interatomic distances between occupants of the anion column must be of reasonable length, 2) the anions must occupy positions found in the structure refinement, and 3) F can occupy a Cl site but Cl cannot occupy an F site because of the resulting short Ca-Cl distances. It is this third criterion that demonstrates how the Cl site at (0,0,0) can exist, and we can rewrite their conclusion #3 for hydroxyl-chlorapatite by substituting “OH” for “F” in their discussion.

Figure 6 depicts an anion sequence in which one Cl_a site (that site at $z = 0, 1/2$) is occupied by a hydroxyl. In that sequence, the presence of that OH allows sufficient distance between that anion and an adjacent Cl_b anion, identical to the mechanism noted for F-Cl apatite by Mackie and Young (1974) and Hughes et al. (2014a, b). Relatively few of the Cl positions are of type Cl_a (< 5%), but, as predicted by Mackie and Young (1974), they do exist. The presence of these sites is effected by a column OH anion occupying a Cl site, yielding an acceptable OH-Cl distance in the anion column; however, all of those sites need not be occupied by OH.

In the anion column of $OH \approx Cl$ apatites, a second Cl site, Cl_b , is found at $z \approx 0.093$, and yields bond distances to three $Ca2'$ atoms of 2.777\AA . An additional site occurs at $z \approx 0.163$. Like the ClOH site in OH-Cl apatites with $OH > Cl$, this site (also labeled ClOH) accommodates *both* Cl and OH, with an OH occupant bonding to $Ca2$ at a distance of 2.404\AA and a Cl occupant bonding to the disordered $Ca2'$ atom at a distance of 2.647\AA . Thus, through the disordering of $Ca2$ to $Ca2'$, as in $OH > Cl$ apatite a single site can accommodate either column anion with acceptable bond distances.

A final site, OH_a , is also present in the OH - Cl binary anion column wherein $\text{OH} \approx \text{Cl}$. That site, at $(0,0,1/4)$, is at a position in the center of the Ca₂ triangle, identical to the position occupied by F in fluorapatite and ternary apatites. In their study of OH-Cl apatites, Garcia-Tunion (2012) found the OH to occupy that site as well, demonstrating that the hydroxyl can occupy the site on the mirror plane that is normally occupied by F. Bond distances from the OH site at $(0,0,1/4)$ to the three Ca₂ atoms in the Ca₂ triangle are 2.351 Å, affording an acceptable (H)O-Ca bond distance.

The site occupied by OH at $(0,0,1/4)$ was a surprise in the structure solutions, as that is a site typically only occupied by F in the apatite anion column, but in retrospect the reason for its existence is obvious. As seen in Figure 6, the OH_a site is essential for reversing the anion column. Without that site the two adjacent column-reversing sites would be occupied by a ClOH below the plane and a ClOH site above the plane, moving down the anion column. These sites would be 2.28 Å apart without the intervening OH_a site, illustrating the structural role of the OH_a site, a novel OH site in the calcium phosphate apatites.

Finally, to further test the veracity of the structure model and the quality of the structure refinements, we noted that, for the structure model with $\text{OH} \approx \text{Cl}$ and $\text{OH} > \text{Cl}$, there should be a relationship between the amount of the disordered Ca₂' vs. the amount of Cl in Cl_b plus the Cl in the ClOH site (Table 6). Because each Cl atom in Cl_b and each Cl atom in the mixed-occupancy ClOH site (calculated as noted previously) bonds to three Ca₂' atoms in the disordered Ca₂ triangle, we plotted the occupancy of $(\text{Ca}_2'/3)$ vs. $(\text{Cl}_b + \text{Cl in ClOH})$. Figure 7 illustrates the relationship, and the R² value of 0.9906 underscores the veracity of the model and the remarkable quality of the structure data, particularly considering the relatively small occupancy of the several column anion sites.

HYDROGEN BONDING IN THE ANION COLUMN

One important aspect to consider when defining the nature of column anion substitution in the apatite structure, where OH is involved, is hydrogen bonding (H-bonding). It is expected (and has been observed in the F-OH binary; Young et al. 1969) that the H associated with the OH in the anion column will form linear strong hydrogen bonds with the neighboring anions in the anion column. Furthermore, as mentioned in previous sections, H-bonding between neighboring column anions is considered essential for the existence of some of the proposed anion-anion distances. The multiple column anion sites observed in each of the three column site arrangements found when $\text{OH} > \text{Cl}$, $\text{Cl} > \text{OH}$ and $\text{OH} \approx \text{Cl}$, combined with many feasible arrangements of these column anion sites, leads to a large number of possible H-bonding environments in the structure of OH-Cl apatites. Table 7 lists all possible O(H)-X distances (X = OH, Cl) distances for $\text{Cl} > \text{OH}$ (Table 1), $\text{OH} > \text{Cl}$ (Table 3), and $\text{OH} \approx \text{Cl}$ (Table 5). Whereas all of the H-bonding environments are considered feasible in Table 7, they may not all actually exist. As mentioned previously in the text, in the $\text{OH} \approx \text{Cl}$ column site variation OH is predicted to occupy the Cl_a and Cl_b sites in a sequence necessary to incorporate Cl at the Cl_a site (Figure 6), thus H-bonding environments are included in table 7 that are a result of this necessary sequence.

Figure 8 depicts the IR spectrum in the OH stretching region of an apatite in our $\text{OH} \approx \text{Cl}$ compositional group ($\approx 3550\text{cm}^{-1}$). As shown therein, and also noted in spectra of Cl-OH apatites with $\text{OH} > \text{Cl}$ and $\text{Cl} > \text{OH}$, there are multiple peaks in the region; the multiple peaks result from the multiple H-bonding environments for the hydroxyl hydrogens. We are currently collecting IR spectra to correlate individual absorption peaks with the individual H-bonding environments in the Cl-OH binary apatite anion column, and will report those subsequently.

IMPLICATIONS

Calcium phosphate apatite is the most abundant phosphate mineral, and a phase with fundamental importance in geology, agriculture, materials science, medicine and dentistry. All hard tissue of the human body except small parts of the inner ear is formed of apatite materials, indicating a remarkable link between the inorganic and organic genesis for the mineral; apatite is among the few most common biominerals on Earth. In addition, apatite forms the foundation of the global phosphorus cycle. The importance of apatite in many disciplines, indeed in even sustaining human life as the chief source of phosphate for fertilizer, cannot be overstated. Despite the overwhelming importance of calcium phosphate apatite, it is remarkable that the details of this mineral are not well known.

This work elucidates the methods of achieving solid solution along the OH-Cl binary in calcium phosphate apatites, and illustrates the complex, compositional dependent nature of the solid solution mechanisms. It also demonstrates that detailed diffraction studies can reveal the fine details of the apatite atomic arrangement and the behavior of atoms in the apatite anion column.

ACKNOWLEDGEMENTS

Support for this work was provided by the National Science Foundation through grant EAR-1249459 to JMH and EAR-0952298 to JR. The manuscript was improved by reviews by Francis McCubbin, an anonymous reviewer, and the *American Mineralogist* Technical Editor, for which we are very appreciative. Aaron Celestian is gratefully acknowledged for the editorial handling of the manuscript.

REFERENCES CITED

- Akella, J., Vaidya, S.N., Kennedy, G.C., (1969) Melting of sodium chloride at pressures to 65 kbar. *Physical Review* 185 (3), 1135–1140.
- Brown, I.D. (1976) On the geometry of O-H...O hydrogen bonds. *Acta Crystallographica*, A32, 24-31.
- Garcia-Tunion, E., Dacuna, B., Zaragoza, G., Franco, J., and Guitian, F. (2012) Cl-OH ion-exchanging process in chlorapatite ($\text{Ca}_5(\text{PO}_4)_3\text{Cl}_x(\text{OH})_{1-x}$) – a deep insight. *Acta Crystallographica*, B68, 467-479.
- Hughes, J.M. (2015) The many facets of apatite. Mineralogical Society of America Presidential Address. *American Mineralogist*, 100, 1033-1039.
- Hughes, J.M., Cameron, M., and Crowley, K.D. (1989) Structural variations in natural F, OH and Cl apatites. *American Mineralogist*, 74, 870-876.
- Hughes, J. M., Cameron, M. and Crowley, K.D. (1990) Crystal structures of natural ternary apatites: solid solution in the $\text{Ca}_5(\text{PO}_4)_3\text{X}$ (X = F, OH, Cl) system. *American Mineralogist*, 75, 295-304.
- Hughes, J.M., Cameron, M., and Crowley, K.D. (1990) Crystal structures of natural ternary apatites: Solid solution in the $\text{Ca}_5(\text{PO}_4)_3\text{X}$ (X = F, OH, Cl) system. *American Mineralogist*, 75, 295-304.
- Hughes, J.M., and Rakovan, J. (2015) Structurally robust, chemically diverse: Apatite and apatite supergroup minerals. *Elements*, 11, 167-172.
- Hughes, J.M., Nekvasil, H., Ustunisik, G., Lindsley, D.H., Coraor, A.E., Vaughn, J., Phillips, B., McCubbin, F.M., and Woerner, W.R. (2014a) Solid solution in the fluorapatite -

- chlorapatite binary system: High-precision crystal structure refinements of synthetic F-Cl apatite. *American Mineralogist* 99, 369-376.
- Hughes, J.M., Heffernan, K.M., Goldoff, B., and Nekvasil, H. (2014b) Fluor-chlorapatite, devoid of OH, from the Three Peaks Area, Utah: The first reported structure of natural fluor-chlorapatite. *Canadian Mineralogist*, 52, 643-652.
- Jenkins, H.D.B., and Thakur, K.P. (1979) Reappraisal of thermochemical radii for complex anions. *Journal of Chemical Education*, 56, 576-577.
- McCubbin, F.M., Mason, H.E., Park, H., Phillips, B.L., Parise, J.B., Nekvasil, H., and Lindsley, D.H. (2008) Synthesis and characterization of low-OH- fluor-chlorapatite: A single-crystal XRD and NMR spectroscopic study. *American Mineralogist*, 93, 210-216.
- Mackie, P. E., and Young, R. A. (1974) Fluorine-chlorine interaction in fluor-chlorapatite. *Journal of Solid State Chemistry*, 11, 319-329.
- Putnis, A. (2009) Mineral replacement reactions. In E.H. Oelkers and J. Schott, Eds., *Thermodynamics and Kinetics of Water-Rock Interaction*, 70, p. 87–124. Reviews in Mineralogy and Geochemistry, Mineralogical Society of America, Chantilly, Virginia.
- Schettler, G., Gottschalk, M., and Harlov, D.E. (2011) A new semi-micro wet chemical method for apatite analysis and its application to the crystal chemistry of fluorapatite-chlorapatite solid solutions. *American Mineralogist*, 96, 138–152.
- Shannon, R.D., and Prewitt, C.T. (1969) Effective ionic radii in oxides and fluorides. *Acta Crystallographica*, B25, 925-946.
- Sheldrick, G.M. (2008) A short history of *SHELX*. *Acta Crystallographica*, A64, 112–122.
- Sudarsanan, K., and Young, R.A. (1978) Structural interactions of F, Cl and OH in apatites. *Acta Crystallographica*, B34, 1401-1407.

Vener, M.V., Shishkina, A.V., Rykounov, A.A., and Tsirelson, V.G. (2013) Cl...Cl interactions in molecular crystals: Insights from the theoretical charge density analysis. *The Journal of Physical Chemistry A*, 117, 8459-8467.

Young, R.A., van der Lugt, W., and Elliott, J.C. (1969) Mechanism for fluorine inhibition of diffusion in hydroxyapatite. *Nature*, 223, 729-730.

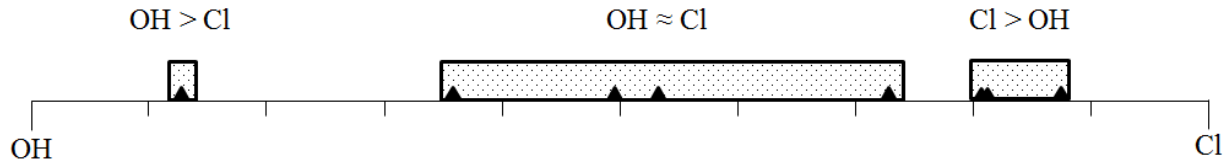


FIGURE 1. Compositions along the calcium phosphate apatite OH-Cl binary studied in this work.

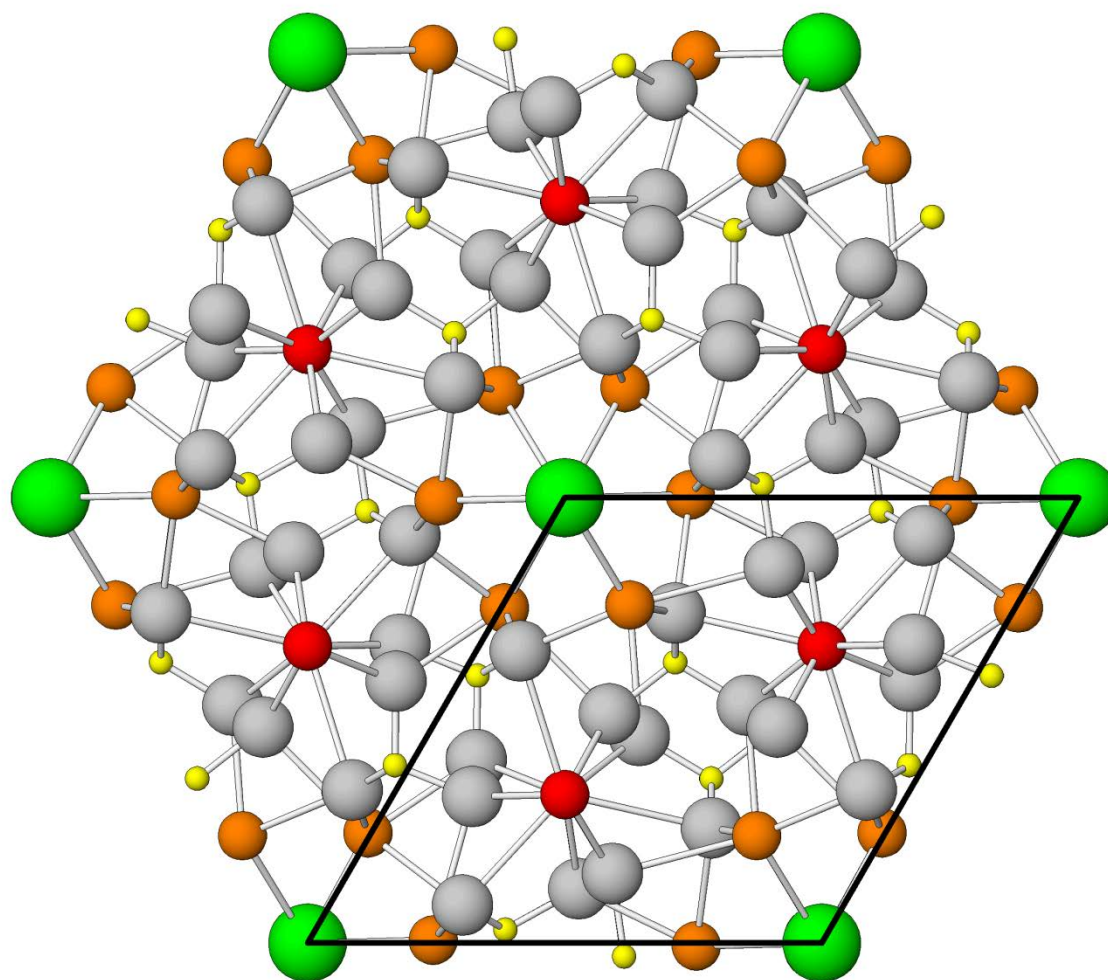


FIGURE 2. The apatite atomic arrangement projected on (001). Green atoms represent projection of anion column, yellow atoms are P, red atoms are Ca1, and orange atoms are Ca2. From Hughes (2015).

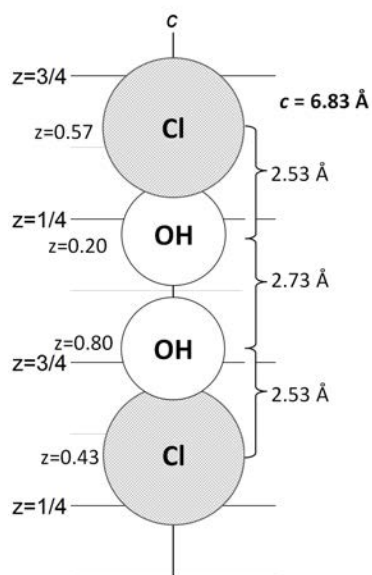


FIGURE 3. Depiction of incompatibility of OH and Cl positions observed in endmember hydroxylapatite and chlorapatite in OH-Cl binary anion column.

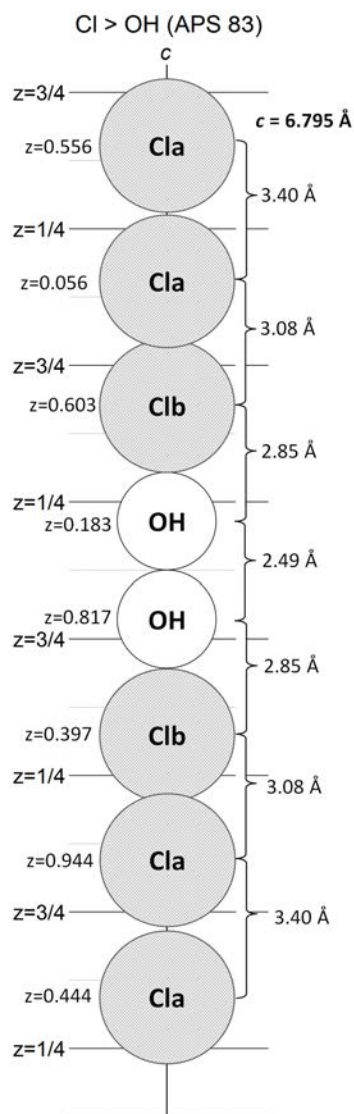


FIGURE 4. Depiction of reversal of anion column in OH-Cl binary calcium phosphate apatites with Cl > OH. The depicted sequence provides sufficient anion-anion distances and allows reversal of anion sequence to preserve $P6_3/m$ symmetry.

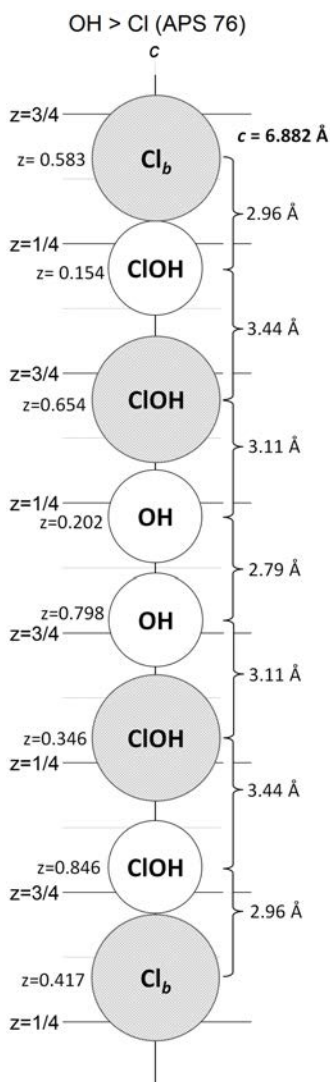


FIGURE 5. Depiction of reversal of anion column in OH-Cl binary calcium phosphate apatites with OH > Cl. The depicted sequence provides sufficient anion-anion distances and allows reversal of anion sequence to preserve $P6_3/m$ symmetry.

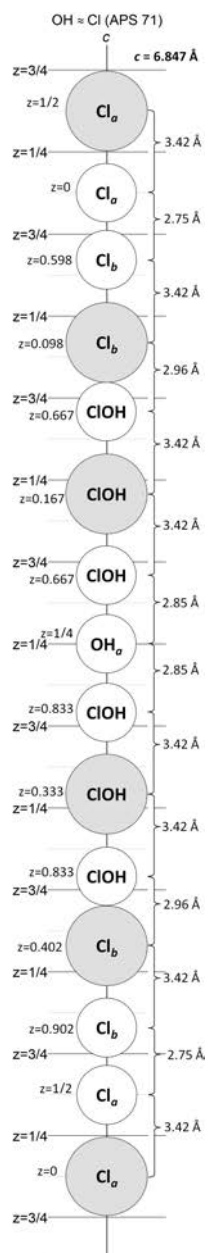


FIGURE 6. Depiction of reversal of anion column in OH-Cl binary calcium phosphate apatites with $\text{OH} \approx \text{Cl}$. The depicted sequence provides sufficient anion-anion distances and allows reversal of anion sequence to preserve $P6_3/m$ symmetry.

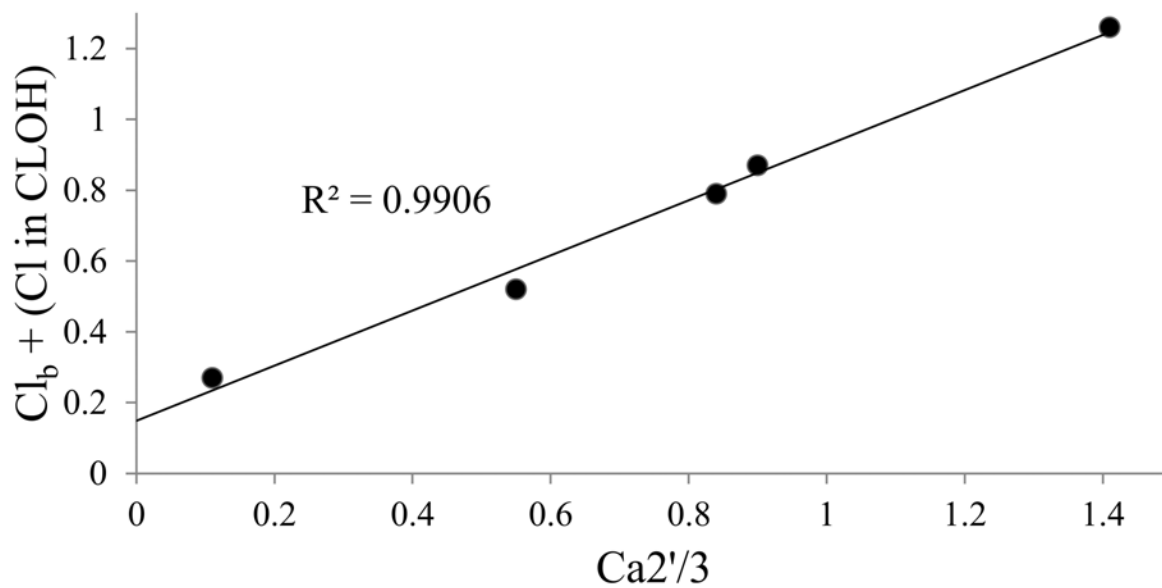


FIGURE 7. Plot of occupancy of $Ca^{2'}/3$ vs. occupancy of $[Cl_b + (Cl \text{ in } ClOH)]$ for $OH \approx Cl$ apatites and $OH > Cl$ apatites. As noted in text, because each Cl bonds to three $Ca^{2'}$ atoms, the relationship should be linear with an intercept of 0.

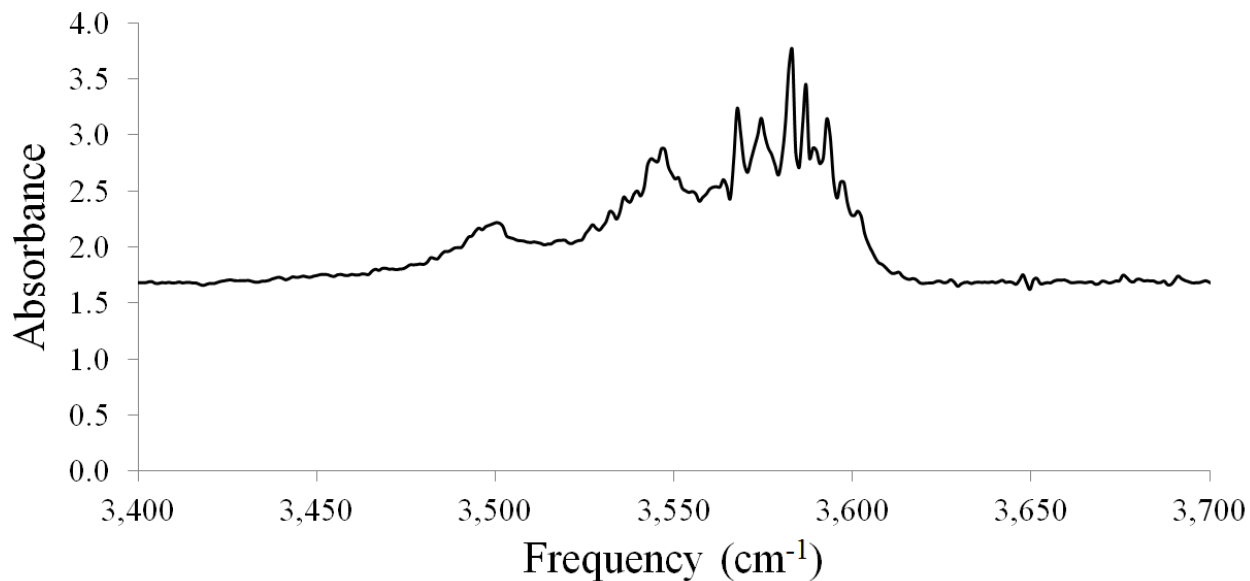


FIGURE 8. IR absorbance in the OH stretching region for APS 72. Multiple peaks are easily distinguishable, supporting the existence of many H-bonding environments in the structure of OH \approx Cl apatites. Similar results were found for OH > Cl apatites and Cl > OH apatites.

TABLE 1. Atomic coordinates and equivalent isotropic atomic displacement parameters (\AA^2) for sample APS83, with Cl > OH.

Atom	x/a	y/b	z/c	U(eq)*
Ca1	2/3	1/3	0.99684(5)	0.01064(8)
Ca2	0.25900(3)	0.00225(3)	1/4	0.01124(8)
P	0.62592(4)	0.03242(4)	1/4	0.00658(8)
O1	0.50913(13)	0.85072(12)	1/4	0.0133(2)
O2	0.53493(13)	0.12661(13)	1/4	0.0147(2)
O3	0.73389(10)	0.08691(10)	0.06748(13)	0.02010(18)
OH	0	0	0.183(5)	0.003(5)
ClB	0	0	0.103(3)	0.0094(16)
ClA	0	0	0.0562(8)	0.0130(6)

*U(eq) is defined as one third of the trace of the orthogonalized U_{ij} tensor.

**Total contents in unit cell.

TABLE 2. Values of z for column anions in (0,0, z) sites and percentage of total column anion occupancy in OH-Cl binary apatites with Cl > OH. Total sites determined by single-crystal site-refinement.

Sample	OH	% Sites	Cl _a	% Sites	Cl _b	% Sites	Column Occ. ¹
APS78	0.183	18.2	0.058	55.1	0.106	26.7	OH _{0.37} Cl _{1.65}
APS82	0.181	18.5	0.061	57.5	0.108	24.0	OH _{0.38} Cl _{1.66}
APS83	0.183	12.8	0.056	62.4	0.103	24.8	OH _{0.26} Cl _{1.75}

TABLE 3. Atomic coordinates and equivalent isotropic atomic displacement parameters (\AA^2) for APS76, with OH > Cl.

Atom	x/a	y/b	z/c	U(eq)
Ca1	2/3	1/3	0.99843(5)	0.00993(8)
Ca2	0.2465(4)	0.99354(6)	1/4	0.0082(2)
Ca2'	0.275(4)	0.9922(13)	1/4	0.0082(2)
P	0.63142(4)	0.03027(4)	1/4	0.00549(8)
O1	0.51529(12)	0.84426(12)	1/4	0.01064(18)
O2	0.53517(13)	0.12240(13)	1/4	0.0140(2)
O3	0.74152(10)	0.08573(10)	0.06994(12)	0.01870(17)
OH	0	0	0.2024(14)	0.0097(10)
ClB	0	0	0.083(13)	0.092(19)
ClOH	0	0	0.154(5)	0.006(5)

*U(eq) is defined as one third of the trace of the orthogonalized U_{ij} tensor.

**Total contents in unit cell.

TABLE 4. Values of z for column anions in (0,0, z) sites and percentage of total column anion occupancy in OH-Cl binary apatites with OH > Cl.

Sample	OH	% Sites	Cl _b	% Sites	ClOH ¹	% Sites	Column Occ ² .
APS76	0.202	84.5	0.083	6.4	0.154	9.1	OH _{1.73} Cl _{0.27}

¹(ClOH site: 21.7 % OH, 78.2% Cl)

²Constrained to 2.00 column anions/formula unit.

TABLE 5. Atomic coordinates and equivalent isotropic atomic displacement parameters (\AA^2) for APS71, with OH \approx Cl.

Atom	x/a	y/b	z/c	U(eq)*
Ca1	2/3	1/3	0.99776(5)	0.01068(8)
Ca2	0.2450(6)	0.9973(5)	1/4	0.0096(4)
Ca2'	0.2676(6)	0.9952(8)	1/4	0.0096(4)
P	0.62959(4)	0.03164(4)	1/4	0.00627(8)
O1	0.51273(13)	0.84771(12)	1/4	0.01273(19)
O2	0.53594(14)	0.12471(13)	1/4	0.0163(2)
O3	0.73802(10)	0.08660(10)	0.06890(13)	0.02171(19)
OHA	0	0	1/4	0.013(3)
ClOH	0	0	0.1667(9)	0.0129(10)
ClA	0	0	0	0.031(7)
ClB	0	0	0.0984(9)	0.0119(11)

*U(eq) is defined as one third of the trace of the orthogonalized U_{ij} tensor.

**Total contents in unit cell.

TABLE 6. Values of z for column anions in (0,0, z) sites and percentage of total column anion occupancy in OH-Cl binary apatites with $\text{OH} \approx \text{Cl}$.

Sample	OH_a	% Sites	Cl_a	% Sites	Cl_b	% Sites	CIOH	% Sites	Column occ.*
APS71	1/4	19.5	0	4.2	0.098	27.4	0.167 ¹	48.9	$\text{OH}_{1.01}\text{Cl}_{0.99}$
APS72	1/4	7.0	0	5.9	0.082	52.5	0.156 ²	34.5	$\text{OH}_{0.53}\text{Cl}_{1.47}$
APS74	1/4	17.7	0	4.0	0.096	30.7	0.164 ³	47.6	$\text{OH}_{0.92}\text{Cl}_{1.08}$
APS80	1/4	25.9	0	3.8	0.096	16.9	0.164 ⁴	53.4	$\text{OH}_{1.30}\text{Cl}_{0.70}$

¹(CIOH site: 63.0 % OH, 37.0% Cl); ²(CIOH site: 56.3 % OH, 43.7% Cl);

³(CIOH site: 60.0 % OH, 40.0% Cl); ⁴(CIOH site: 72.8 % OH, 27.2% Cl).

*Constrained to $(\text{OH}+\text{Cl}) = 2.00$.

TABLE 7. List of the theoretical H-bonding environments that may possibly exist for each structural type, using APS 71, 76, and 83 as models. OH...O represents H-bonding to a neighboring O anion, and OH...Cl represents H-bonding to a neighboring Cl anion. The site column and the neighbor column represent the two anion sites that when placed next to each other in the column yield the corresponding anion-anion distance listed. The $Cl_b - Cl_a$, $Cl_b - Cl_b$, and $Cl_a - Cl_a$ H-bonding environments in the $OH \approx Cl$ compositional range are predicted to exist, likely at low occupancy.

	O-H...O			O-H...Cl		
	Anion-Anion Distance (Å)	Site	Neighbor	Anion-Anion Distance (Å)	Site	Neighbor
OH ≈ Cl, APS 71	3.42	CIOH	CIOH	3.42	CIOH	CIOH
	4.56	CIOH	CIOH	4.56	CIOH	CIOH
	2.85	CIOH	OHa	3.89	CIOH	Clb
	3.99	CIOH	OHa	2.96	CIOH	Clb
	3.42	OHa	OHa	5.03	CIOH	Clb
				4.46	OHa	Clb
				3.99	OHa	CIOH
	2.75	Clb	Clb	3.42	Clb	Clb
				3.42	Clb	Clb
OH > Cl, APS 76	O-H...O			O-H...Cl		
	Anion-Anion Distance (Å)	Site	Neighbor	Anion-Anion Distance (Å)	Site	Neighbor
	3.44	CIOH	CIOH	3.44	CIOH	CIOH
	4.77	CIOH	CIOH	4.77	CIOH	CIOH
	3.11	CIOH	OH	3.11	CIOH	OH
	3.78	CIOH	OH	3.78	CIOH	OH
	4.43	CIOH	OH	4.43	CIOH	OH
	2.45	CIOH	OH	3.93	CIOH	Clb
	2.79	OH	OH	2.96	CIOH	Clb
4.10	OH	OH	4.26	OH	Clb	
3.44	OH	OH	4.92	OH	Clb	
Cl > OH, APS 83	O-H...O			O-H...Cl		
	Anion-Anion Distance (Å)	Site	Neighbor	Anion-Anion Distance (Å)	Site	Neighbor
	3.40	OH	OH	4.26	OH	Clb
	2.49	OH	OH	5.17	OH	Clb
	4.30	OH	OH	3.94	OH	Clb
			2.85	OH	Clb	
			4.85	OH	Clb	